
CRITICAL COUPLING VORTEX WITH GRATING-INDUCED HIGH QUALITY OPTICAL TAMM STATES

A PREPRINT

Rashid G. Bikbaev

Kirensky Institute of Physics, Federal Research Center KSC SB RAS, Krasnoyarsk 660036, Russia
Siberian Federal University, Krasnoyarsk 660041, Russia

Dmitrii N. Maksimov

Kirensky Institute of Physics, Federal Research Center KSC SB RAS, Krasnoyarsk 660036, Russia
Siberian Federal University, Krasnoyarsk 660041, Russia

Pavel S. Pankin

Kirensky Institute of Physics, Federal Research Center KSC SB RAS, Krasnoyarsk 660036, Russia
Siberian Federal University, Krasnoyarsk 660041, Russia

Kuo-Ping Chen

Institute of Imaging and Biomedical Photonics, National Chiao Tung University, 71150 Tainan, Taiwan

Ivan V. Timofeev

Kirensky Institute of Physics, Federal Research Center KSC SB RAS, Krasnoyarsk 660036, Russia
Siberian Federal University, Krasnoyarsk 660041, Russia

January 25, 2022

ABSTRACT

We investigate optical Tamm states supported by a dielectric grating placed on top of a distributed Bragg reflector. It is found that under certain conditions the Tamm state may become a bound state in the continuum. The bound state, in its turn, induces the effect of critical coupling with reflectance amplitude reaching an exact zero. We demonstrate that the critical coupling point is located in the core of a vortex of the reflection amplitude gradient in space of wavelength and angle of incidence. The emergence of the vortex is explained by the coupled mode theory.

The combination of plasmon and photon structures leads to hybrid systems, which have been of great interest over the recent few years. One example of such a hybrid system is a two-dimensional lattice of nanoparticles combined with a Fabry-Perot resonator [1, 2]. The unique properties of such systems can be applied to narrowband absorbers [3, 4], lasers [5, 6], sensors [7, 8] and photodetectors [9]. The hybrid systems are used to reduce losses in plasmonics [10] and for local amplification of the electromagnetic field [11].

Hybrid two-dimensional lattices not only act as structural elements but can also be used as mirrors for engineering localized states. It is recently shown [12] that a Tamm plasmon (TP) [13] can be excited at the interface between binary Au nanodisk arrays and distributed Bragg reflector (DBR). In this case coupling between the TP and localized lattice resonance mode results in dual Tamm states. The described structure can be used to measure the Zak phase. Thus in [14] the Zak phase has been determined through the interface state. The propagation of the Tamm plasmons was investigated in [15] by depositing metallic stripes on top of a semiconductor Bragg mirror. It was shown that the TPs are coupled to surface plasmons arising at the stripe edges. These plasmons form an interference pattern close to the bottom surface of the stripe resulting in a change of both the energy and loss rate for the TP. The disadvantage of the hybrid systems is material losses. Therefore, dielectric metasurfaces are increasingly used. For example in [16] the authors

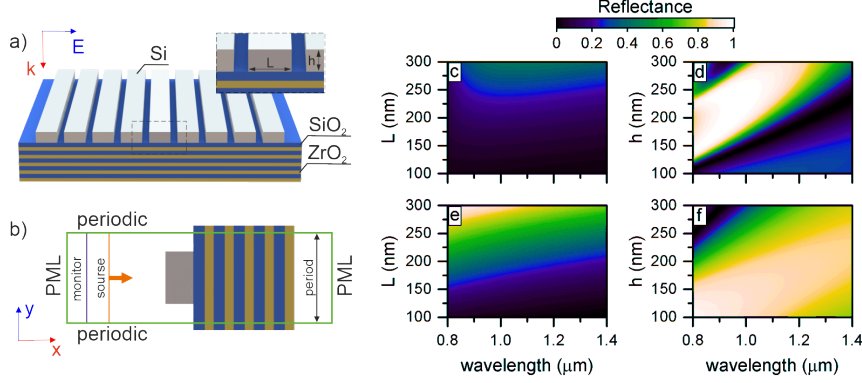


Figure 1: (a) Schematic representation of the structure. (b) Sketch view of the simulation box. Reflectance spectra of the 2D silicon (c,d) and gold (e,f) stripes array for different value of thickness L (c,e) ($h = 100$ nm) and h (d,f) ($L = 300$ nm). Period of the array $p = 400$ nm.

propose narrowband perfect absorbers with enormously high fabrication tolerance, which consist of a low-contrast grating and a finite DBR layer with an ultrathin absorbing medium (graphene). A planar array of optical band-pass filters composed of low loss dielectric metasurface layers sandwiched between two DBRs is reported in [17].

In this paper we demonstrate the advantage of Bragg reflection over total internal reflection. We show that optical Tamm states (OTS) have better quality factor in comparison with TP and surface plasmon resonance. This is because of the absence of material losses and larger resonant volume due to Bragg reflectors [18]. Ultimately, in dielectric structure the OTS can obtain infinite quality factor, i.e. the OTS becomes optical bound state in the continuum (BIC) [19]. Such states supported by dielectric gratings have been previously reported both experimentally [20, 21] and theoretically [22, 23]. Here we demonstrate that the Tamm BIC induces the effect of critical coupling (CC). We show that the CC corresponds a phase singularity in the space of incidence angle and frequency, while the phase gradient forms a vortex with the CC point in the core. The phase singularities carry a topological charge [24] defined as the number of 2π windings of the phase along a closed contour around the CC point. Based on the temporal coupled mode theory [25] we provide semi-analytic expression for the reflection amplitudes that matches with full-wave numerical simulations. The CC points are known to lead to very fast local variation of the phase of the reflection amplitude [26]. Here we find that such fast variation in the vicinity of the CC is unavoidable due to the phase singularity.

Let us consider a DBR with a 2D array of silicon nanostripes on top (Fig. 1a). The DBR unit cell is formed of two layers: silica dioxide (SiO₂) with thickness $d_a = 165$ nm and permittivity $\epsilon_a = 2.1$, and zirconium dioxide (ZrO₂) with thickness $d_b = 135$ nm and permittivity $\epsilon_b = 4.16$. The 2D structure with thickness h and width L has infinite length along y axis with period p . The direction of the incident light on the structure and its polarization are shown by the red and blue arrows, respectively. The optical properties of the structures have been calculated by commercial Finite-Difference Time-Domain (FDTD) package. Standard numerical protocols are implemented to mimic infinite 2D periodic structures. The simulation box is shown in figure 1b.

A localized state, such as OTS, can be formed at the boundary of reflecting media. In our structure, reflection from a DBR is provided by the photonic band gap. If the number of layers is infinite the layered DBR forms an ideal Bragg reflector [27] which prohibits radiation losses. Reflection from the 2D structure can be controlled by varying the lattice period, as well as the thickness and width of the nanostripes. First we calculated the reflectance spectra of the bare 2D structure without a DBR. The simulation results are shown in figure 1(c-f).

The calculations were carried out in two steps. First, we fixed the height of the stripes and varied their width. Thus, the width at which the most reflection from the structure is achieved was determined. In the next step, we varied the height of the stripe with fixed width. In this way, we were able to determine the parameters of the structure at which the largest reflection from the structure can be achieved. The calculation results showed that the largest reflection is achieved in the range from 800 to 1200 nm for a structure with a stripes thickness $h = 250$ nm and a width of $L = 300$ nm (see Fig. 1(c,d)). We also calculated the reflectance spectra of a 2D array of gold stripes. The results are presented in the figure 1(e,f), which shows that the structure reflects in the entire range of wavelengths investigated, but the reflectance is not high, and reaches only 60-70%. We determined that the reflection reaches the maximum value for stripes with thickness $h = 150$ nm and width $L = 300$ nm.

We expect that conjugation of the periodic structures with a DBR could lead to the formation of localized states. To verify this the reflectance spectra of the composite structures were calculated (see Fig. 2). Figure 2a shows that DBR

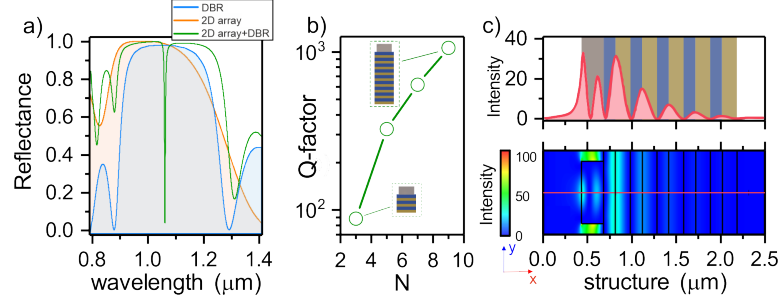


Figure 2: (a) Reflectance spectra of the structure. (b) The Q-factor of the OTS depends on the number of DBR layers and (c) field distribution at the OTS wavelength.

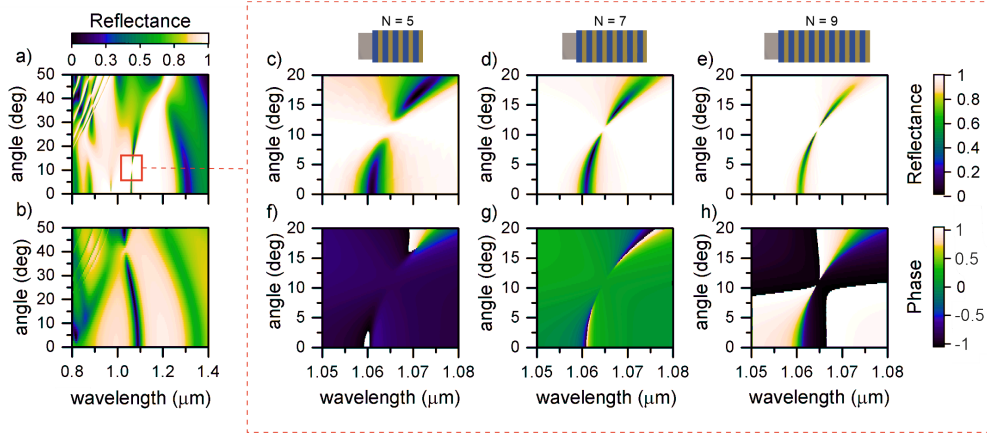


Figure 3: Reflectance spectra of the structure in case of (a) silicon and (b) gold stripes. (c,d,e) Reflectance spectra and (f,g,h) reflection phase of the DBR bounded by 2D silicon stripes for different number of DBR periods.

band gap is in the range of wavelengths from 900 to 1100 nm overlaps with the reflection region of a 2D silicon stripes structure. In the area of their overlap, a narrow spectral line ($\lambda = 1060$ nm) is observed within the photonic band gap. This line corresponds to a state localised at the interface between DBR and 2D array of silicon stripes.

It is important to note that an increase in the number of periods of the DBR leads to a significant increase in the Q-factor of the resonance (see Fig. 2b). Thus, when increasing N from 3 to 9, the Q-factor grows by more than an order of magnitude. This is because the increase in the number of periods of the DBR leads to a decrease of the energy relaxation rate in the lower half-space (the transmission channel of the DBR). When the DBR is infinite, the losses into the lower half-space are totally suppressed by the photonic band gap, whereas the losses to the upper half-space are suppressed by interference [27]. Thus, the OTS becomes a BIC at a specific incidence angle $\theta \approx 10.9^\circ$.

The distribution of the field intensity at the wavelength of the localized state is shown in the figures 2c. One can see that the field is localized close to the interface between the two constituent subsystems and exponentially decreases in the photonic crystal and the 2D lattice. However, unlike conventional OTS, in our case the field is also localized on the front border of the 2D medium. It is interesting to note that the maximum intensity of the field is achieved not in the center of the stripe, but at its boundaries (see bottom subplot in Fig. 2c). This leads to enhancement of the field in the inter-stripe space.

The angular dependencies of the reflectance spectra are shown in the figure 3. The figure shows that the spectra of the localized state for DBR bounded by 2D silicon or gold structure are cardinally different (see Fig. 3(a,b)). The difference is not only in the width of the resonance, but also in the shifting inside the photonic band gap. So, for gold stripes, the localized state is shifted to the blue, same as the conventional TP, while for silicon stripes structure, we observe a red shift. Moreover, in both cases, we see the collapse of the resonant lines, with the only difference that for silicon stripe structure, this effect is observed at lower angles. Let's look at the dielectric structure in more detail. We calculated the reflection spectra of the structure and phase of the reflected wave in the region of the collapse of the resonance line. The calculation results are shown in figures 3(c-h).

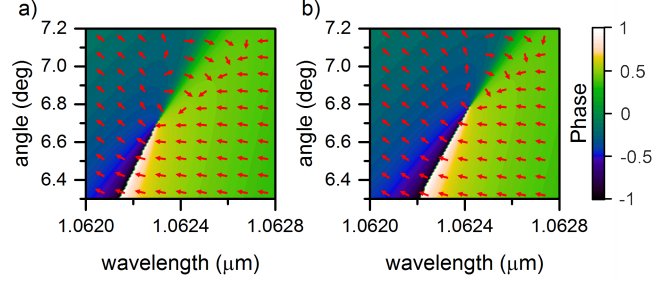


Figure 4: Reflection phase of the DBR bounded by 2D lattice for $N=7$ obtained by (a) FDTD and (b) coupled mode theory. The red arrows represent the direction of the phase gradient.

It can be seen from the reflection spectra that an increase of N leads to the contraction of the resonant lines in the BIC point. It is important to note that for $N = 5$ (see Fig. 3f) only one critical coupling point is observed, while for $N = 7$ and $N = 9$ (see Fig. 3(g,h)) two critical coupling points are present. As the calculations have shown, even at $N = 9$, we do not see merging of the two CC points. Further increase of N up to infinity will allow us to achieve this effect, but in this case we would have the problem both with simulations and experimental implementation. Nevertheless, we see that the variation of N in the specified interval allowed us to demonstrate this effect.

The scattering spectrum in the vicinity of a localized state can be described in the framework of the temporal coupled mode theory [25]. According to the temporal coupled mode theory the reflection amplitude can be written as follows

$$r = e^{i2\eta} \left(-1 + \frac{2\gamma_1(\theta)}{i[\omega - \bar{\omega}(\theta)] + \gamma_1(\theta) + \gamma_2} \right), \quad (1)$$

where ω is the frequency of the incident wave, $\bar{\omega}$ - the resonant frequency, η - global phase, θ - the angle of incidence, and $\gamma_{1,2}$ are the inverse life-times due to coupling to the upper and lower half-spaces, correspondingly. Notice, that we ignored the dependence of γ_2 on θ as the coupling to the lower half-space is equally suppressed by the DBR stop band at all angles of incidence. In the upper half-space though, the coupling is cancelled by destructive interference only if $\theta = \theta_{\text{BIC}}$. By setting $r = 0$ one immediately arrives at the condition for the CC

$$\begin{aligned} \omega &= \bar{\omega}(\theta_{\text{CC}}), \\ \gamma_2 &= \gamma_1(\theta_{\text{CC}}). \end{aligned} \quad (2)$$

Since we have two parameters to satisfy the two equations above the CCs are points in the plane of θ and ω . One can immediately see from Eq. (2) that in case of a true BIC, $N = \infty$ and $\gamma_2 = 0$ the two CC points merge with the BIC. The dispersion of the entries of Eq. (1) are given by [28]

$$\begin{aligned} \bar{\omega} &= \omega_0 - \alpha\theta^2 + \mathcal{O}(\theta^4), \\ \gamma_1 &= \beta(\theta^2 - \theta_{\text{BIC}}^2)^2 + \mathcal{O}(\theta^6), \end{aligned} \quad (3)$$

where we took into account the symmetry of the leaky band about the Γ -point. Equation (3) contains two unknowns, α and β . The first, α , can be easily found by fitting to the Lorentzian center-frequency in Fig. 3d. The second parameter, β , can be derived as

$$\beta = \frac{\gamma_2}{(\theta_{\text{CC}}^2 - \theta_{\text{BIC}}^2)^2}, \quad (4)$$

$2\gamma_2$ being the half-width of the Lorentzian at the CC angle. The phase singularity manifests itself in the vortical behaviour of the gradient of the phase, ϕ [24] of the reflection coefficient in space of θ and ω . The phase ϕ in Eq. (5) is implicitly defined via $r = |r|e^{i\phi}$. Although the phase is not uniquely defined due to 2π windings around the CC point, the gradient is a well-behaved function and, thus, can be derived analytically from Eq. (1), by using the following equation

$$\nabla\phi = \frac{r^*\nabla r - r\nabla r^*}{2i|r|^2}. \quad (5)$$

We spare the reader of the cumbersome equations resulting from substitution of Eq. (1) into Eq. (5). Notice, though, that since the global phase η is independent of both θ and λ it is absent from Eq. (5).

In Fig. 4 we compare the results obtained with Eq. (5) against the results of full-wave numerical simulations. The figure shows the phase of the wave reflected from the structure and the direction of the phase gradient near one of the critical

coupling points. It should be noted that the results are in good agreement and critical coupling vortices are observed in both cases.

In summary, we have demonstrated that the critical coupling effect induced by a Tamm BIC is associated with a phase singularity of the reflection coefficient in the space of wavelength and angle of incidence of the impinging plane wave. The scattering spectrum is explained by a single resonance coupled mode approach. The resulting equation is found to correctly account of the topological property of the critical coupling vortex. We speculate that the results presented open novel opportunities in engineering critical coupling, whereas the phase singularity yields unlimited sensitivity to variation of the system's parameters paving a way to sensing applications.

Acknowledgment

This work was co-funded by RFBR, project no. 19-52-52006, and the Taiwan Ministry of Science and Technology, project no. 108-2923E-009-003-MY3.

References

- [1] Ralf Ameling and Harald Giessen. Microcavity plasmonics: strong coupling of photonic cavities and plasmons. *Laser & Photonics Reviews*, 7(2):141–169, 3 2013.
- [2] V.S. Gerasimov, A.E. Ershov, R.G. Bikbaev, I.L. Rasskazov, I.V. Timofeev, S.P. Polyutov, and S.V. Karpov. Engineering mode hybridization in regular arrays of plasmonic nanoparticles embedded in 1D photonic crystal. *Journal of Quantitative Spectroscopy and Radiative Transfer*, 224:303–308, 2 2019.
- [3] Debashis Chanda, Kazuki Shigeta, Tu Truong, Eric Lui, Agustin Mihi, Matthew Schulmerich, Paul V. Braun, Rohit Bhargava, and John A. Rogers. Coupling of plasmonic and optical cavity modes in quasi-three-dimensional plasmonic crystals. *Nature Communications*, 2(1):477–479, 2011.
- [4] Zhengqi Liu, Guiqiang Liu, Xiaoshan Liu, Shan Huang, Yan Wang, Pingping Pan, and Mulin Liu. Achieving an ultra-narrow multiband light absorption meta-surface via coupling with an optical cavity. *Nanotechnology*, 26(23):235702, 6 2015.
- [5] Wei Zhou, Montacer Dridi, Jae Yong Suh, Chul Hoon Kim, Dick T Co, Michael R Wasielewski, George C Schatz, and Teri W Odom. Lasing action in strongly coupled plasmonic nanocavity arrays. *Nature Nanotechnology*, 8(7):506–511, 6 2013.
- [6] Andreas Mischok, Mona Kliem, Robert Brückner, Stefan Meister, Hartmut Fröb, Malte C. Gather, and Karl Leo. Phase-locked lasing in 1d and 2d patterned metal-organic microcavities. *Laser & Photonics Reviews*, 12(8):1800054, June 2018.
- [7] Mohsen Bahramipanah, Shourya Dutta-Gupta, Banafsheh Abasahl, and Olivier J F Martin. Cavity-Coupled Plasmonic Device with Enhanced Sensitivity and Figure-of-Merit. *ACS Nano*, 9(7):7621–7633, 7 2015.
- [8] Jing Chen, Qian Zhang, Cheng Peng, Chaojun Tang, Xueyang Shen, Licheng Deng, and Gun-sik Park. Optical Cavity-Enhanced Localized Surface Plasmon Resonance for High-Quality Sensing. *IEEE Photonics Technology Letters*, 30(8):728–731, 4 2018.
- [9] R. J. Thompson, T. Siday, S. Glass, T. S. Luk, J. L. Reno, I. Brener, and O. Mitrofanov. Optically thin hybrid cavity for terahertz photo-conductive detectors. *Applied Physics Letters*, 110(4):041105, January 2017.
- [10] Ryosuke Kamakura, Shunsuke Murai, Satoshi Ishii, Tadaaki Nagao, Koji Fujita, and Katsuhisa Tanaka. Plasmonic-Photonic Hybrid Modes Excited on a Titanium Nitride Nanoparticle Array in the Visible Region. *ACS Photonics*, 4(4):815–822, 4 2017.
- [11] Salma Alrasheed and Enzo Di Fabrizio. Effect of Surface Plasmon Coupling to Optical Cavity Modes on the Field Enhancement and Spectral Response of Dimer-Based sensors. *Scientific Reports*, 7(1):10524, 12 2017.
- [12] Li Wang and Yongyuan Jiang. Confined dual hybrid states through coupling Tamm plasmon and localized lattice resonance. In Hongxing Xu, Satoshi Kawata, and David J. Bergman, editors, *Plasmonics III*, volume 10824, pages 26 – 31. International Society for Optics and Photonics, SPIE, 2018.
- [13] M Kaliteevski, I. Iorsh, S. Brand, R. A. Abram, J. M. Chamberlain, A. V. Kavokin, and I. A. Shelykh. Tamm plasmon-polaritons: Possible electromagnetic states at the interface of a metal and a dielectric Bragg mirror. *Physical Review B*, 76(16):165415, 10 2007.
- [14] Qiang Wang, Meng Xiao, Hui Liu, Shining Zhu, and C. T. Chan. Measurement of the zak phase of photonic bands through the interface states of a metasurface/photonic crystal. *Phys. Rev. B*, 93:041415, Jan 2016.

- [15] I. Yu. Chestnov, E. S. Sedov, S. V. Kutrovskaya, A. O. Kucherik, S. M. Arakelian, and A. V. Kavokin. One-dimensional tamm plasmons: Spatial confinement, propagation, and polarization properties. *Phys. Rev. B*, 96:245309, Dec 2017.
- [16] Sangjun Lee, Hyungjun Heo, and Sangin Kim. High fabrication-tolerant narrowband perfect graphene absorber based on guided-mode resonance in distributed bragg reflector. *Scientific Reports*, 9(1), March 2019.
- [17] Yu Horie, Amir Arbabi, Ehsan Arbabi, Seyede Mahsa Kamali, and Andrei Faraon. Wide bandwidth and high resolution planar filter array based on DBR-metasurface-DBR structures. *Optics Express*, 24(11):11677, May 2016.
- [18] C. Symonds, S. Azzini, G. Lheureux, A. Piednoir, J. M. Benoit, A. Lemaitre, P. Senellart, and J. Bellessa. High quality factor confined tamm modes. *Scientific Reports*, 7(1), June 2017.
- [19] Chia Wei Hsu, Bo Zhen, A. Douglas Stone, John D. Joannopoulos, and Marin Soljačić. Bound states in the continuum. *Nature Reviews Materials*, 1(9):16048, Jul 2016.
- [20] Zarina F. Sadrieva, Ivan S. Sinev, Kirill L. Koshelev, Anton Samusev, Ivan V. Iorsh, Osamu Takayama, Radu Malureanu, Andrey A. Bogdanov, and Andrei V. Lavrinenko. Transition from optical bound states in the continuum to leaky resonances: Role of substrate and roughness. *ACS Photonics*, 4(4):723–727, Mar 2017.
- [21] Hugo M. Doeleman, Francesco Monticone, Wouter den Hollander, Andrea Alù, and A. Femius Koenderink. Experimental observation of a polarization vortex at an optical bound state in the continuum. *Nature Photonics*, 12(7):397–401, June 2018.
- [22] E. N. Bulgakov, D. N. Maksimov, P. N. Semina, and S. A. Skorobogatov. Propagating bound states in the continuum in dielectric gratings. *Journal of the Optical Society of America B*, 35(6):1218–1222, may 2018.
- [23] Evgeny N. Bulgakov and Dmitrii N. Maksimov. Avoided crossings and bound states in the continuum in low-contrast dielectric gratings. *Physical Review A*, 98(5):053840, nov 2018.
- [24] Konstantin Y Bliokh, Miguel A Alonso, and Mark R Dennis. Geometric phases in 2d and 3d polarized fields: geometrical, dynamical, and topological aspects. *Reports on Progress in Physics*, 82(12):122401, oct 2019.
- [25] Shanhui Fan, Wonjoo Suh, and J. D. Joannopoulos. Temporal coupled-mode theory for the fano resonance in optical resonators. *Journal of the Optical Society of America A*, 20(3):569, mar 2003.
- [26] Yoichiro Tsurumaki, Jonathan K. Tong, Victor N. Boriskin, Alexander Semenov, Mykola I. Ayzatsky, Yuri P. Machekhin, Gang Chen, and Svetlana V. Boriskina. Topological engineering of interfacial optical tamm states for highly sensitive near-singular-phase optical detection. *ACS Photonics*, 5(3):929–938, jan 2018.
- [27] Chia Wei Hsu, Bo Zhen, Song-Liang Chua, Steven G Johnson, John D Joannopoulos, and Marin Soljačić. Bloch surface eigenstates within the radiation continuum. *Light Sci Appl*, 2(7):e84, Jul 2013.
- [28] Evgeny N. Bulgakov and Dmitrii N. Maksimov. Topological bound states in the continuum in arrays of dielectric spheres. *Physical Review Letters*, 118(26):267401, jun 2017.